Inorganic Chemistry

Article

pubs.acs.org/IC

Relationship between Gallium Pyramidalization in L·$GaCl_3$ Complexes and the Electronic Ligand Properties

Ahmad El-Hellani,[†] Julien Monot,[†] Shun Tang,[†] Régis Guillot,[†] Christophe Bour,[†] and Vincent Gandon*[,†,‡]

[†]ICMMO (UMR CNRS 8182), Université Paris Sud, 91405 Orsay Cedex, France

[‡]ICSN-CNRS, Bat 27-1 avenue de la Terrasse, 91198 Gif-sur-Yvette Cedex, France

Supporting Information

ABSTRACT: Six new molecular $GaCl_3$ adducts of electron rich compounds of the *carbone* (carbodiphosphorane, tetraaminoallene) and cyclic alkyl amino carbene (CAAC) families have been synthesized and characterized by X-ray crystallography. The sum of their Cl−Ga−Cl angles has been compared to those of 20 other complexes exhibiting various oxygen-, nitrogen-, phosphorus-, and carbon-donor ligands for which good quality X-ray analyses have been reported. The pyramidalization of the $GaCl_3$ moiety in L·$GaCl_3$ complexes has been checked against the computed antisymmetric stretching of the Ga−Cl bonds. It has also been compared to the symmetric stretching of the C−O bonds of the corresponding L·$Ni(CO)_3$ complexes (Tolman Electronic Parameter). On this basis, a relationship between the pyramidalization observed in the gallium complexes and the electronic ligand properties has been established.

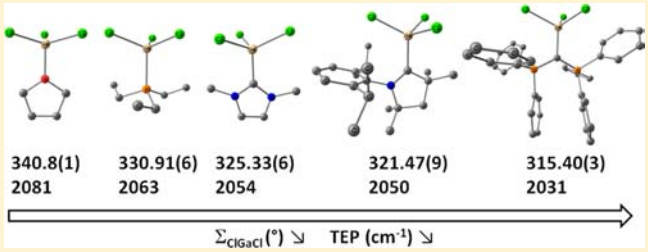

INTRODUCTION

The ability of Group 13 donor−acceptor complexes[1] to activate small molecules,[2] store hydrogen,[3] and promote or catalyze various organic transformations[4,5] is attracting increased attention. In homogeneous catalysis, the use of complexes instead of simple inorganic salts usually improves the stability and the solubility of the Lewis acids, as well as the selectivity of the reaction. Making the right choice of ligand is a crucial issue for controlling the formation, the stability, and the reactivity of the active species. Quantitative descriptions of all kinds of ligands are available, but they mostly derive from spectroscopic analyses of transition metal complexes. These methods generally capture the net bonding between the ligand and the metal fragment which includes σ,π-donation, π-acceptance, and steric effects.[6] However, the π-acceptor property is not relevant for main group metals.[7] On the other hand, the first and second proton affinities (PAs)[8] capture the σ- and the π-donor properties respectively, but ignore steric effects. Our work on gallium catalysis[9] led us to look for a descriptor that would specifically quantify ligand properties in L·$GaCl_3$ adducts. We have recently disclosed that complexes of type $[L{\cdot}GaCl_2]^+$, which are obtained by treatment of L·$GaCl_3$ with a silver salt, are valuable catalysts able to imitate gold or platinum complexes in some cycloisomerization reactions (Scheme 1). The success of these transformations depends on the nature of the ligand which facilitates or retards the chlorine abstraction step by modulating the strength of the Ga−Cl bond in the neutral precatalyst, and tunes the Lewis acidity of the active cationic species. For instance, whereas PPh_3 or 3,5-lutidine complexes only provide trace amount of product, high efficiency can be reached with the IPr N-heterocyclic carbene (NHC).

Scheme 1. Ligand Effect in Ga(III)-Catalyzed Cycloisomerization/Friedel-Crafts Tandem

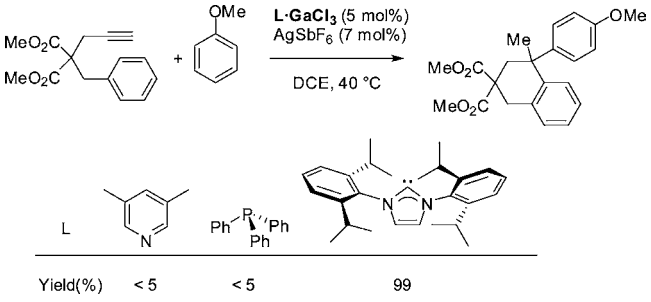

Comparison of (NHC)·$GaCl_3$[10] with ether, phosphine oxide, phosphine, or amine adducts that are described in the literature shows that net differences exist in the solid state geometry of the $GaCl_3$ moiety and in the wavenumbers of the Ga−Cl infrared bands (vide infra).

To get a larger view and validate the use of such descriptors for evaluating ligands properties, the synthesis of complexes exhibiting ligands that are more electron rich than NHCs is needed. Among such ligands, carbon(0) derivatives (also referred to as *carbones*),[11] and cyclic alkyl amino carbenes (CAACs)[11c,d] are relevant choices since their distinct properties

Received: July 15, 2013
Published: September 26, 2013

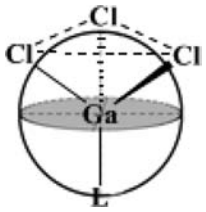

compared to NHCs have been exploited in π-acid catalysis.[12,13] Carbodiphosphoranes and carbodicarbenes are typical *carbones*. They display bent allene structures which can be conveniently represented as phosphine- or carbene-stabilized C(0)-derivatives with two lone pairs at the central carbon (Scheme 2, entries (1) and (2)).[14] This rendition highlights the reactivity of these compounds toward Lewis acids such as gold chloride for which both the mono- and the digold complexes of hexaphenylcarbodiphosphorane have been synthesized (entry (3)).[15]

Scheme 2. Resonance Forms of Prototypical Carbodiphosphoranes (1) and Carbodicarbenes (2), and Examples of Mono- and Digold Complexes of Hexaphenylcarbodiphosphorane (3)

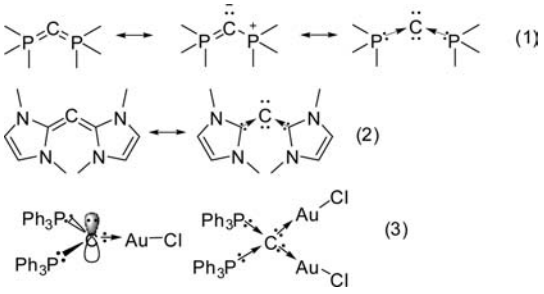

As far as gallium complexes are concerned, only two 1:1 adducts of the quite particular mixed *carbones* **1** and **2** (Chart 1) with $GaCl_3$ have been reported.[16] To complete the collection, we chose to use the carbodiphosphorane **3**,[17] the cyclic carbodiphosphorane **4**,[18] and the tetraaminoallene **5**.[19] While **3** and **4** display bent structures that easily qualify them as *carbones*, **5** is a normal linear allene. However, it is known to behave as a masked carbon(0)-derivative,[20] a prototype of carbodicarbene.[20d] Compound **3** is probably the most emblematic member of the *carbone* family. A variety of transition- and main group metal complexes has been synthesized with this ligand,[11b] yet none with gallium. In Group 13, three adducts have been described: **3**-BH_3,[7a] **3**-$InMe_3$, and **3**-$AlBr_3$.[21] As for the cyclic carbodiphosphorane **4**, only three complexes have been reported: **4**-BH_3, **4**-$ZnMe_2$, and **4**-$CdMe_2$.[18b] To the best of our knowledge, tetraaminoallenes have been used as ligands only once to synthesize [**5**-$AuPPh_3$]SbF_6.[20d] Regarding the CAACs, no gallium complexes have been reported. Among Group 13 elements, only boron has received attention.[22]

We describe herein the synthesis and characterization of six molecular L·$GaCl_3$ adducts where L is a *carbone* or a CAAC. The comparison of their peculiar geometries with some reported complexes encouraged us to study the relationship between the pyramidalization at the metal center and the electronic ligand properties. This structural parameter is checked against computed IR wavenumbers of the Ga−Cl bonds, IR wavenumbers of the C−O bonds of the corresponding L$Ni(CO)_3$ complexes (TEP), and the proton affinity (PA) of the free ligand.

EXPERIMENTAL SECTION

Materials and Instrumentation. All reactions were performed in oven-dried flasks under a positive pressure of argon. Commercially available reagents were used as received without further purification. Gallium(III) chloride was obtained from Alfa Aesar. Dichloromethane was distilled from calcium hydride, diethyl ether and tetrahydrofuran were distilled from sodium/benzophenone ketyl. ^{1}H, ^{13}C, and ^{31}P NMR spectra were recorded on Bruker spectrometers. Chemical shifts are given in ppm. ^{1}H and ^{13}C spectra were calibrated to the residual signals of the solvent. Data are represented as follows: chemical shift, multiplicity, coupling constant (J) in Hz, and integration. HRMS were performed on a MicrOTOFq Bruker spectrometer. Infrared spectra were recorded on a FTIR Perkin-Elmer Spectrum 100 spectrometer.

Synthesis of 3-, 4-, and 5-$GaCl_3$. To a solution of *carbone* (0.5 mmol) in tetrahydrofuran (THF, 7 mL) was added gallium(III) chloride (88 mg, 0.5 mmol) in one portion at room temperature (rt). The reaction mixture was stirred overnight during which a powder precipitated. The complex was isolated after filtration and washings with THF. Single crystals were grown by slow diffusion of diethyl ether to a dichloromethane solution of the gallium complex.

3-GaCl₃. Isolated as a white powder (300 mg, 85% yield). mp = 244−246 °C; ^{1}H NMR (300 MHz, CD_2Cl_2) δ 7.70−7.62 (m, 8 H), 7.53−7.44 (m, 12 H), 7.38−7.33 (m, 10 H); ^{13}C NMR (75 MHz, CD_2Cl_2) δ 134.3, 132.8, 129.4, 128.3; ^{31}P NMR (121 MHz, CD_2Cl_2): δ 23.4; HRMS (ESI) m/z: Calcd for $C_{37}H_{30}Cl_3GaNaP_2$ $[M+Na]^+$: 733.0042, Found: 733.0036. IR (Nujol): ν_{Ga-Cl} = 393 (s), 367 (m), 344 (m), 327 (m) cm^{-1}.

4-GaCl₃. Isolated as a beige powder (135 mg, 45% yield). ^{1}H NMR (300 MHz, CD_2Cl_2): δ 7.78−7.71 (m, 12 H), 7.67−7.60 (m, 8 H), 2.79 (m, 4 H), 2.48−2.44 (m, 2 H); ^{13}C NMR (75 MHz, CD_2Cl_2): δ 133.2, 131.5, 129.5, 128.3, 23.36, 17.0; ^{31}P NMR (121 MHz, CD_2Cl_2) δ 13.3. HRMS (ESI) m/z: Calcd for $C_{28}H_{27}P_2$ $[M-GaCl_3]^+$: 425.1585, Found: 425.1613. IR (Nujol): ν_{Ga-Cl} overlapped.

5-GaCl₃. Isolated as a white powder (111 mg, 57% yield). mp = 149−151 °C; ^{1}H NMR (300 MHz, CD_2Cl_2) δ 3.01 (s, 24 H); ^{13}C NMR (75 MHz, CD_2Cl_2) δ 174.1, 169.2, 41.7; HRMS (ESI) m/z: Calcd for $C_{11}H_{24}Cl_3GaN_4Na$ $[M+Na]^+$: 409.0220, Found: 409.0215. IR (Nujol): ν_{Ga-Cl} = 375 (s, br), 362 (s, br), 336.0 (m, br), 313 (m, br) cm^{-1}.

Chart 1. Carbon-Based Ligands of the *carbone* (1−5) and CAAC Families

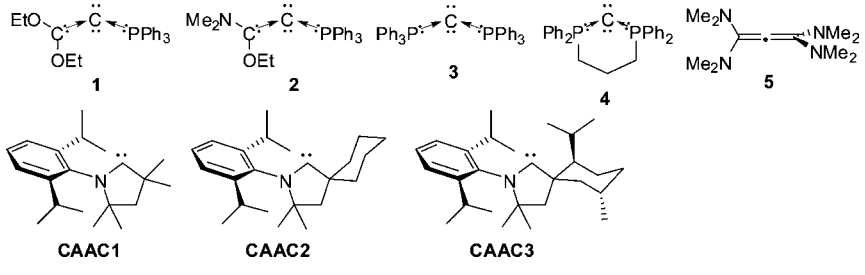

dx.doi.org/10.1021/ic401817g | Inorg. Chem. 2013, 52, 11493−11502

Table 1. Crystal Structure Information

	3-$GaCl_3$	4-$GaCl_3$	5-$GaCl_3$	CAAC1-$GaCl_3$	CAAC2-$GaCl_3$	CAAC3-$GaCl_3$
empirical formula	$C_{37}H_{30}Cl_3GaP_2$	$C_{28}H_{26}Cl_3GaP_2$, CH_2Cl_2	$C_{11}H_{24}Cl_3GaN_4$	C_{20} $H_{31}Cl_3GaN$	$C_{23}H_{35}Cl_3GaN$	$C_{27}H_{43}Cl_3GaN$
M_r	712.62	685.42	388.41	461.53	501.59	557.69
crystal size, mm^3	0.33 × 0.19 × 0.19	0.24 × 0.20 × 0.17	0.24 × 0.21 × 0.08	0.33 × 0.28 × 0.25	0.32 × 0.31 × 0.26	0.13 × 0.04 × 0.02
crystal system	monoclinic	monoclinic	orthorhombic	orthorhombic	monoclinic	orthorhombic
space group	$P2_1/c$	$P2_1//n$	$Pna2_1$	$P2_12_12_1$	$P2_1$	$P2_12_12_1$
a, Å	15.8249(8)	11.8128(4)	15.3185(7)	9.2801(3)	9.3208(3)	9.0024(10)
b, Å	11.5094(6)	15.2735(6)	8.0781(3)	9.5188(3)	14.9396(6)	16.1231(17)
c, Å	18.4355(8)	16.6469(5)	27.4363(13)	25.2707(9)	9.7467(4)	18.953(2)
α, deg	90	90	90	90	90	90
β, deg	109.4220(10)	96.6300(10)	90	90	115.5110(10)	90
γ, deg	90	90	90	90	90	90
cell volume, $Å^3$	3166.7(3)	2983.39(18)	3395.1(3)	2232.30(13)	1224.89(8)	2751.0(5)
Z; Z'	4 ; 1	4 ; 1	8 ; 2	4 ; 1	2 ; 1	4 ; 1
T, K	100(1)	100(1)	100(1)	100(1)	100(1)	100(1)
F_{000}	1456	1392	1600	960	524	1176
μ, mm^{-1}	1.250	1.496	2.086	1.595	1.460	1.307
θ range, deg	1.36−37.46	1.82−36.39	1.48−30.51	1.61−37.36	2.32−36.35	1.66−26.41
reflection collected	39 691	40 867	50 202	24 389	18 717	37 022
reflections unique	13 396	9 839	10 013	10 107	8 743	5 635
R_{int}	0.0292	0.0273	0.0595	0.0488	0.0187	0.1091
GOF	1.065	1.023	1.059	1.075	0.937	0.965
refl. obs. ($I > 2\sigma(I)$)	10 488	8 385	8 417	8 770	8 193	4 144
parameters	388	334	359	234	259	299
wR_2 (all data)	0.0908	0.0814	0.0635	0.1234	0.0481	0.1190
R value ($I > 2\sigma(I)$) Flack parameter	0.0331/	0.0301/	0.0319 0.006(7)	0.0456 0.080(9)	0.0211 0.009(4)	0.0510 0.000(15)
largest diff. peak and hole (e $Å^{-3}$)	−0.518; 0.971	−1.190; 1.686	−0.421; 0.439	−0.817; 0.961	−0.302; 0.615	−0.817; 1.079

Synthesis of CAAC1-, CAAC2-, and CAAC3-$GaCl_3$. Dry THF was added at −78 °C to a 1:1 mixture of LDA and the iminium salt.[23] The suspension was warmed to rt and stirred for 30 min. After removal of the volatiles, the solid residue was suspended in dry hexane. Gallium trichloride was added at −25 °C, and the reaction mixture was allowed to stand at rt overnight. After evaporation of the solvent, the gallium complex was precipitated in methanol as a white solid. Slow evaporation of $CDCl_3$ in the NMR tube afforded crystals suitable for X-ray diffraction analysis.

CAAC1-GaCl₃. Isolated as a white solid (86 mg, 41%). mp = 146−148 °C; ^{1}H NMR (360 MHz, $CDCl_3$) δ 7.49 (t, J = 7.5 Hz, 1 H), 7.31 (d, J = 7.5 Hz, 2 H), 2.67 (sept, J = 7.75 Hz, 2 H), 2.20 (s, 2 H), 1.81 (s, 6 H), 1.51 (s, 6 H), 1.36 (d, J = 6.5 Hz, 6 H), 1.33 (d, J = 6.5 Hz, 6 H); ^{13}C NMR (63 MHz, $CDCl_3$) δ 144.9, 131.0, 125.9, 83.8, 55.7, 50.6, 29.1, 26.3, 24.7. HRMS (ESI) m/z: Calcd for $C_{20}H_{31}Cl_3GaNNa$ $[M+Na]^+$: 482.1170; Found: 482.0644. IR (Nujol): ν_{Ga-Cl} = 385 (s, br), 365 (s, br) cm^{-1}.

CAAC2-GaCl₃. Isolated as a white solid (53 mg, 42%). mp = 202−205 °C; ^{1}H NMR (300 MHz, $CDCl_3$) δ 7.50 (t, J = 7.5 Hz, 1 H), 7.32 (d, J = 8.1 Hz, 2 H), 2.82−2.64 (m, 5 H), 2.3 (s, 2 H), 1.93−1.88 (m, 2 H), 1.80−1.70 (m, 3 H), 1.52 (s, 6 H), 1.46−1.40 (m, 3 H), 1.38 (d, J = 6.6 Hz, 6 H), 1.34 (d, J = 6.6 Hz, 6 H); ^{13}C NMR (90 MHz, $CDCl_3$) δ 145.0, 131.7, 130.9, 125.8, 83.7, 61.4, 44.8, 34.9, 29.7, 29.1, 26.3, 24.7, 24.5, 21.8; HRMS (ESI) m/z: Calcd for $C_{23}H_{35}Cl_2GaN$ $[M-Cl]^+$: 464.1397; Found: 464.1478. IR (Nujol): ν_{Ga-Cl} = 376 (m, br) cm^{-1}.

CAAC3-GaCl₃. Isolated as a white solid (73 mg, 70%). mp = 213-215 °C. $[\alpha]_D^{20}$ = +8.2 (c = 1.0 in $CHCl_3$). ^{1}H NMR (300 MHz, $CDCl_3$) δ 7.47 (t, J = 7.7 Hz, 1 H), 7.34 (d, J = 7.7 Hz, 1 H), 7.28 (d, J = 7.7 Hz, 1H), 2.81 (sept, J = 6.4 Hz, 1 H), 2.64 (d, J = 13.6 Hz, 2 H), 2.58−2.49 (m, 5 H), 2.07 (d, J = 13.6 Hz, 2 H), 2.04−1.95 (m, 2 H), 1.67−1.59 (m, 1 H), 1.44 (d, J = 6.5 Hz, 3 H), 1.39 (d, J = 6.5 Hz, 3 H), 1.46−1.40 (m, 3 H), 1.38 (d, J = 6.6 Hz, 3 H), 1.32 (s, 6 H); 1.29 (s, 3 H); 1.07 (d, J = 6.6 Hz, 3 H), 1.02 (d, J = 6.7 Hz, 3 H), 0.93 (d, J = 6.6 Hz, 3 H). ^{13}C NMR (90 MHz, $CDCl_3$) δ 145.3, 145.1, 130.8, 126.8, 125.5, 81.3, 66.8, 56.3, 53.0, 50.5, 33.8, 32.3, 29.5, 29.2, 28.7, 28.6, 27.4, 26.0, 24.9, 24.4, 22.7, 22.1, 21.5. HRMS (ESI) m/z: Calcd for $C_{27}H_{43}Cl_2GaN$ $[M-Cl]^+$: 520.2023; Found: 520.2323. IR (Nujol): ν_{Ga-Cl} = 375 (m, br) cm^{-1}.

X-ray Analyses. X-ray diffraction data was collected using a Kappa X8 APPEX II Bruker diffractometer with graphite-monochromated $Mo_{K\alpha}$ radiation (λ = 0.71073 Å). Crystals were mounted on a CryoLoop (Hampton Research) with Paratone-N (Hampton Research) as cryoprotectant and then flash-frozen in a nitrogen gas stream at 100 K. The temperature of the crystal was maintained at the selected value (100 and 200 K) by means of a 700 series Cryostream cooling device (accuracy of ±1 K). The data were corrected for Lorentz polarization and absorption effects. Semiempirical absorption corrections were applied. The structures were solved by direct methods using SHELXS-97[24] and refined against F^2 by full-matrix least-squares techniques using SHELXL-97[25] with anisotropic displacement parameters for all non-hydrogen atoms. Hydrogen atoms were located on a difference Fourier map and introduced into the calculations as a riding model with isotropic thermal parameters. All calculations were performed by using the Crystal Structure crystallographic software package WINGX.[26] The absolute configuration was determined by refining the Flack's parameter using a large number of Friedel's pairs.[27] The crystal data collection and refinement parameters are given in Table 1. CCDC 947075−947080 contains the supplementary crystallographic data for this paper. These data can be obtained free of charge from the Cambridge Crystallographic Data Centre via http://www.ccdc.cam.ac.uk/Community/Requestastructure/.

Quantum-Chemical Computations. Optimizations were carried out using the Gaussian '03 software package.[28] For the calculation of the PAs, the MP2[29]/def2-TZVPP//BP86[30]/def2-SVP[31] level of theory was used as described.[32] For the evaluation of the Tolman Electronic Parameter (TEP), $LNi(CO)_3$ complexes were optimized using the mPW1PW91/6-311+G(2d) (Ni)/6-311+G(d,p) (other atoms) level of theory[33] or the BP86/def2-SVP level of theory.[34] For the gallium

dx.doi.org/10.1021/ic401817g | Inorg. Chem. 2013, 52, 11493−11502

complexes, the BP86/def2-SVP level of theory was used. Stationary points were characterized as minima by calculating the Hessian matrix analytically at this level of theory. The $\%V_{bur}$[35] were obtained through the Samb*V*ca@MoLNaC Web site (https://www.molnac.unisa.it/OMtools/sambvca.php) using the ligand coordinates derived from the X-ray analysis of the L·$GaCl_3$ complexes. The center of the sphere was located at 2.0 Å from the donor atom. H atoms were omitted, except for secondary amines. Average values were calculated when two molecules were found existing in the unit cell.

RESULTS AND DISCUSSION

We started with the synthesis of donor–acceptor complexes of $GaCl_3$ with *carbones*. The desired products could be obtained (see Experimental Section for details), and single crystals suitable for X-ray diffraction could be grown (Figures 1–3,

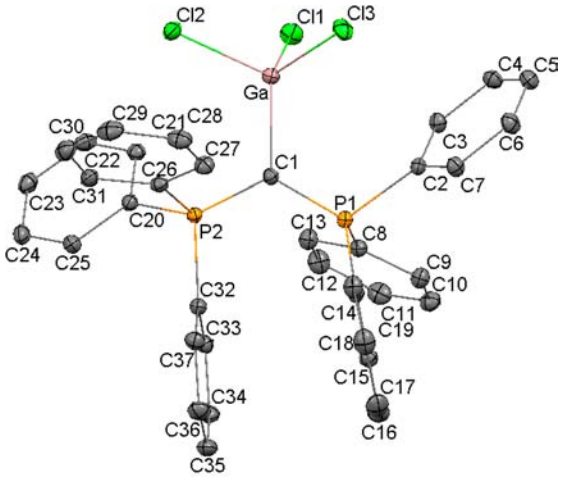

Σ_{CGaCl} (°) 340.5(1); Σ_{ClGaCl} (°) 315.40(3)

Figure 1. Molecular structure of **3-$GaCl_3$** in the crystal (thermal ellipsoids at 50% probability level; hydrogen atoms omitted for clarity). Selected interatomic distances (Å): Ga–C1 1.981(1), Ga–Cl1 2.2277(4), Ga–Cl2 2.2089(4), Ga–Cl3 2.1821(3), C1–P1 1.713(1), C1–P2 1.714(1). Selected bond angles (deg): Cl1–Ga–Cl2 104.11(1), Cl1–Ga–Cl3 107.40(1), Cl2–Ga–Cl3 103.89(1), C1–Ga–Cl1 111.59(4), C1–Ga–Cl2 113.86(4), C1–Ga–Cl3 115.09(4), P1–C1–P2 122.46(7).

Table 1). While the unit cells of **3**- and **4-$GaCl_3$** consist of single molecules, that of **5-$GaCl_3$** contains two enantiomers, which is consistent with the fact that bent allene complexes can be helically chiral.[36] In **3**- and **4-$GaCl_3$**, the P–C1 bond distances are virtually the same (1.714 Å). On the other hand, the P–C1–P angle is, as one would expect, more acute in the cyclic carbodiphosphorane derivative (116.70(8) vs 122.46(7)). The C1–Ga bond is longer in **3-$GaCl_3$** than in **4-$GaCl_3$** (1.981(1) vs 1.947(1)). In **5-$GaCl_3$**, the C1–C2 bond is shorter than the C1–C3 bond (1.396(4) vs 1.437(4) Å). On the side of the shortest one, the C–N bonds are longer than on the other side (1.366(3) vs 1.350(3)). This dissymmetry is less pronounced in the reported gold complex (C–C 1.424(5) vs 1.407(5) Å; C–N 1.366(5) vs 1.370(av)).[20d] The exceptional pyramidalization of the $GaCl_3$ moiety in **3**-, **4**-, and **5-$GaCl_3$** is striking. The sum of the C–Ga–Cl angles is 340.5(1)°, 342.9(1)°, and 344.2(2)° respectively, and reciprocally, the sum of the Cl–Ga–Cl angles is 315.40(3)°, 312.64(3)°, and 310.85(8)°. A search in the Cambridge Crystallographic Database for donor–acceptor adducts of $GaCl_3$ in which the sum of the E–Ga–Cl (E = C, N, O, P) angles is close to 340°

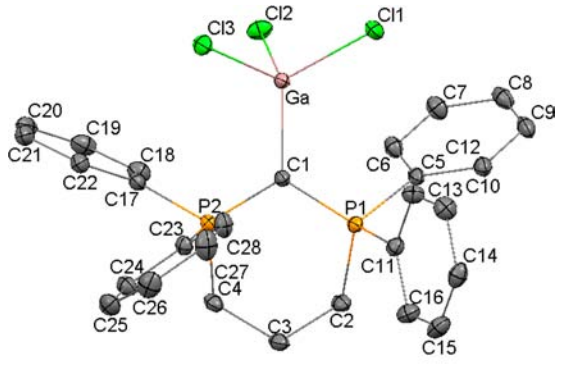

Σ_{CGaCl} (°) 342.9(1); Σ_{ClGaCl} (°) 312.64(3)

Figure 2. Molecular structure of **4-$GaCl_3$** in the crystal (thermal ellipsoids at 50% probability level; hydrogen atoms omitted for clarity). Selected interatomic distances (Å): Ga–C1 1.947(1), Ga–Cl1 2.2082(4), Ga–Cl2 2.2216(4), Ga–Cl3 2.2142(3), C1–P1 1.715(1), C1–P2 1.713(1). Selected bond angles (deg): Cl1–Ga–Cl2 103.67(1), Cl1–Ga–Cl3 104.03(1), Cl2–Ga–Cl3 104.94(1), C1–Ga–Cl1 117.90(4), C1–Ga–Cl2 114.44(4), C1–Ga–Cl3 110.58(4), P1–C1–P2 116.70(8).

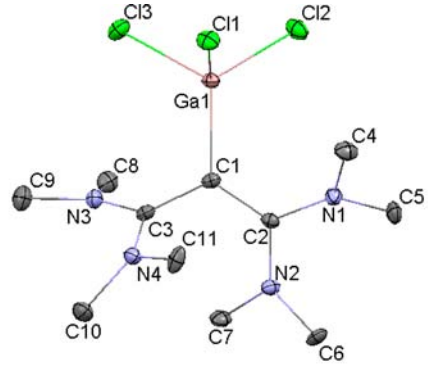

Σ_{CGaCl} (av, °) 344.2(2); Σ_{ClGaCl} (av, °) 310.85(8)

Figure 3. Molecular structure of **5-$GaCl_3$** in the crystal (thermal ellipsoids at 50% probability level; hydrogen atoms omitted for clarity). Selected interatomic distances (Å): Ga1–C1 1.965(2), Ga1–Cl1 2.2497(7), Ga1–Cl2 2.2036(6), Ga1–Cl3 2.2155(7), C1–C2 1.396(4), C1–C3 1.437(4). Selected bond angles (deg): Cl1–Ga1–Cl2 106.56(2), Cl1–Ga1–Cl3 99.68(3), Cl2–Ga1–Cl3 104.48(3), C1–Ga1–Cl1 111.37(8), C1–Ga1–Cl2 116.48(8), C1–Ga1–Cl3 116.58(8), C2–C1–C3 119.7(2).

yielded only a few anionic alkyls and aryls of type $RGaCl_3^-$, as well as the aforementioned complex **2-$GaCl_3$** (Σ_{CGaCl} 339.8°; Σ_{ClGaCl} 316.0°). The Σ_{CGaCl} observed in **5-$GaCl_3$** is actually the largest reported for a neutral ligand, the Σ_{ClGaCl} being the smallest.

Next, we synthesized the first $GaCl_3$ adducts of CAACs (see Experimental Section for details). CAACs are known to be strong donors, yet less than *carbones*.[11c] The structure of the gallium complexes could be established by means of X-ray crystallography (Figures 4–6, Table 1). Looking at the CAAC backbone, the solid state structures of **CAAC1-**, **CAAC2-**, and **CAAC3-$GaCl_3$** feature similar bond parameters with those

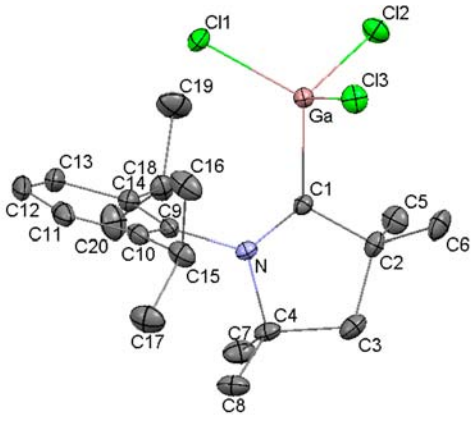

Σ_{CGaCl} (°) 334.8(2); Σ_{ClGaCl} (°) 321.47(9)

Figure 4. Molecular structure of **CAAC1-GaCl$_3$** in the crystal (thermal ellipsoids at 50% probability level; hydrogen atoms omitted for clarity). Selected interatomic distances (Å): Ga−C1 2.039(2), Ga−Cl1 2.1604(8), Ga−Cl2 2.1880(6), Ga−Cl3 2.1910(7), C1−N 1.303(3), C1−C2 1.516(3). Selected bond angles (deg): Cl1−Ga−Cl2 107.47(3), Cl1−Ga−Cl3 107.00(3), Cl2−Ga−Cl3 107.00(3), C1−Ga−Cl1 118.62(6), C1−Ga−Cl2 109.48(6), C1−Ga−Cl3 106.72(6), N−C1−C2 110.9(2).

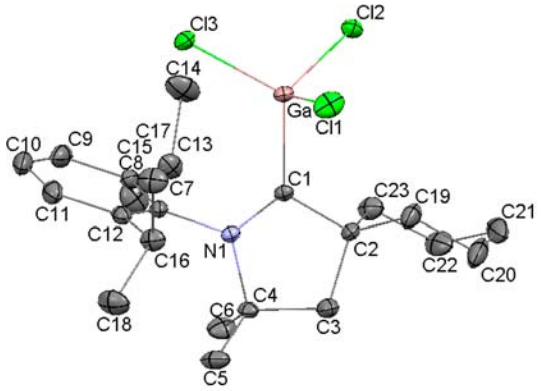

Σ_{CGaCl} (°) 332.31(9); Σ_{ClGaCl} (°) 324.09(3)

Figure 5. Molecular structure of **CAAC2-GaCl$_3$** in the crystal (thermal ellipsoids at 50% probability level; hydrogen atoms omitted for clarity). Selected interatomic distances (Å): Ga−C1 2.036(1), Ga−Cl1 2.1862(4), Ga−Cl2 2.1815(3), Ga−Cl3 2.1730(4), C1−N1 1.293(2), C1−C2 1.521(2). Selected bond angles (deg): Cl1−Ga−Cl2 108.85(1), Cl1−Ga−Cl3 107.39(1), Cl2−Ga−Cl3 107.85(1), C1−Ga−Cl1 103.14(3), C1−Ga−Cl2 110.30(3), C1−Ga−Cl3 118.87(3), N−C1−C2 110.6(1).

previously described with boron.[22] The pyramidalization of the $GaCl_3$ moiety (Σ_{ClGaCl} 321.47(9)°, 324.09(3)°, 318.9(2)° respectively) is quite large but clearly less pronounced than in **3-**, **4-**, and **5-GaCl$_3$**.

Most methods used for the classification of ligands according to their electronic properties rely on liquid phase spectroscopy, especially IR and NMR.[37] In particular, the Tolman Electronic Parameter (TEP),[37a] which corresponds to the A1 symmetrical CO stretching mode (ν_{CO}(A1)) of LNi(CO)$_3$ complexes in CH_2Cl_2, is one of the most popular. The difficulty to achieve the synthesis of such nickel carbonyls led to the development of related scales using LM(CO)$_2$Cl complexes (M = Rh, Ir).[37c] Since these methods implement transition metals, they capture the subtle balance between the σ,π-donor and π-acceptor

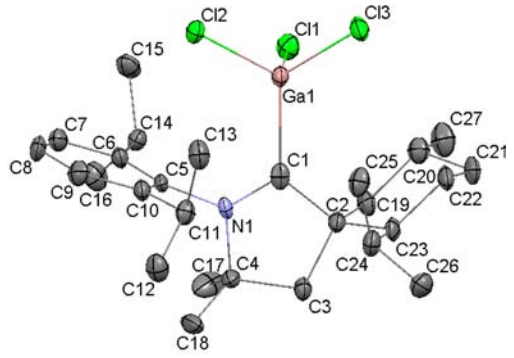

Σ_{CGaCl} (°) 337.5(3); Σ_{ClGaCl} (°) 318.9(2)

Figure 6. Molecular structure of **CAAC3-GaCl$_3$** in the crystal (thermal ellipsoids at 50% probability level; hydrogen atoms omitted for clarity). Selected interatomic distances (Å): Ga1−C1 2.064(5), Ga1−Cl1 2.208(1), Ga1−Cl2 2.179(1), Ga1−Cl3 2.176(1), C1−N1 1.308(7), C1−C2 1.538(8). Selected bond angles (deg): Cl1−Ga1−Cl2 109.83(5), Cl1−Ga1−Cl3 105.87(5), Cl2−Ga1−Cl3 103.17(5), C1−Ga1−Cl1 103.3(1), C1−Ga1−Cl2 116.1(1), C1−Ga1−Cl3 118.1(1), N−C1−C2 110.0(4).

properties of the ligand.[37n] In principle, the chemical shift of the donor atom and of the ^{71}Ga (or ^{69}Ga) nucleus should reflect the electronic ligand properties in L·GaCl$_3$.[38] However, because of the quadrupole moment of the gallium isotopes, their resonances have large line widths in C_{3v} adducts and the nucleus coupled to gallium is difficult to observe. In L·GaCl$_3$, IR bands corresponding to the antisymmetric stretching of the Ga−Cl bond can be very strong and easy to identify if not overlapped with those from the internal vibrations of the ligands (~400 cm^{-1}).[39] Yet they are not always sharp enough to allow a precise measurement, especially with unsymmetrical ligands which split the degenerate modes. The geometries discussed above raised the question whether the solid state structures of L·GaCl$_3$ could be used to establish a scale of the electronic ligand properties. Since crystal packing, non covalent interactions, and crystal forces influence the conformation of flexible molecules,[40] and also because it is sometimes difficult to obtain the precise position of the atoms in a crystal, it would seem inappropriate to base such a scale on X-ray diffraction analysis. However, Timoshkin et al. reported that solid state structures reflect Lewis acidity trends of heavier Group 13 halides. Such analysis must be made with care because the hydrogen bonding network can affect the donor−acceptor bond distance and lead to erroneous conclusions.[41]

According to Bent's rule,[42] for main group elements, the atomic s character tends to concentrate in orbitals directed toward electropositive groups, while the atomic p character tends to concentrate in orbitals directed toward electronegative groups. Thus, for a L·GaCl$_3$ complex, the angles between the chlorine atoms should be smaller than tetrahedral (sp^{3+x} hybridization of the orbitals directed toward Cl, sp^{3-x} hybridization for the orbitals directed toward L).[43] We decided to study the influence of L on the Cl−Ga−Cl angles. In addition to the six gallium species discussed above, the following set of complexes was used for this investigation: ***t*BuPCl$_2$-**,[44] **THF-**,[45] **Me$_3$SiN$_3$-**,[46] **N$_3$P$_2$-**,[47] **3,5-Me$_2$Py-**,[48] **Pip-**, **DMAP-**,[49] ***i*Pr$_2$NH-**,[50] **PEt$_3$-**,[51] **PPr$_3$-**,[52] **NBN-**,[53] **diMe-IDM-**,[10c] **SIPr-**,[9b] **IPr-**,[10b] **IiPrMe$_2$-**,[10b] **1-**, and **2-GaCl$_3$**[16] (see Chart 2 for the structure of the ligands). This set was

dx.doi.org/10.1021/ic401817g | Inorg. Chem. 2013, 52, 11493−11502

Chart 2. Ligands Arranged According to Their TEP (cm^{-1})[a]

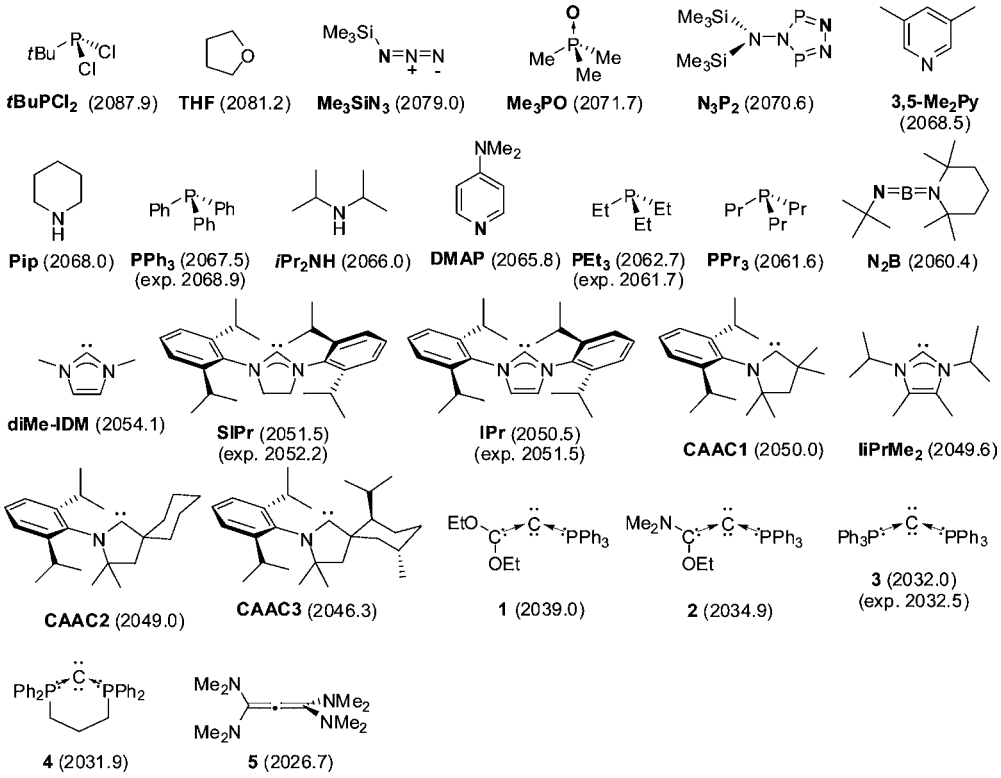

[a]The coordinating atom is highlighted when needed.

limited to complexes displaying relatively simple ligands that were published after 1990, with *R*-factors lower than 5% and limited disorder. Since these criteria considerably reduced the number of phosphines and ruled out phosphine oxides, exceptions were made for **Ph_3P-$GaCl_3$** and **Me_3PO-$GaCl_3$** for which *R*-factors of 6.01% and 5.41% were respectively reported.[54]

The ligands have been arranged in Chart 2 according to their calculated TEP. Because the experimental TEP in CH_2Cl_2 (or $CHCl_3$) is available for only a few of them (PPh_3, PEt_3,[55] SIPr, IPr,[56] **3**[57]), we used the computational method described by Gusev which proved to accurately predict the experimental values for a variety of phosphines and NHCs.[33] Exceptions to the Gusev method were made for the carbodiphosphoranes **3** and **4**. Tonner and Frenking showed that a better agreement with the experimental values could be obtained with another computational approach well-suited for this class of compounds.[34,58] According to the TEP, three families emerge: (*i*) the least donating ligands which are the O-, P-, and N-donors, (*ii*) the strong donors comprising the NHCs and the CAACs, and (*iii*) the very strong donors of the *carbone* family. The relevance of the computed TEP can be noted in the pyridine series for which the donating aptitude follows the expected order (**3,5-Me_2Py** < **DMAP**),[59] as well as in the phosphine series (***t*BuPCl$_2$** < **PPh_3** < **PEt_3** < **PPr_3**). As for the carbon donors, the classification obtained by the calculated TEP follows that derived from the rhodium- and the iridium-scales[37c] in CH_2Cl_2 or $CHCl_3$ (Rh (ν_{CO}^{av}, cm^{-1}): **diMe-IDM** (2044.5)[60] < **IPr** (2037.5)[61] < **IiPrMe$_2$** (2036.0)[62] < **CAAC2** (2035.5);[63] Ir (ν_{CO}^{av}, cm^{-1}): **diMe-IDM** (2025.0) < **SIPr** (2024.9) < **IPr** (2023.9) < **CAAC1** (2020.4) < **CAAC3** (2013.0)).[37] The prediction based on the Ir-scale that SIPr is slightly less electron donating than **IPr** is contradicted by the experimental TEP (ν_{CO}(A1), cm^{-1}): **IPr** (2051.5) < **SIPr** (2052.2).[56] In fact, because of the narrow range of the wavenumbers, each scale shows that it is difficult to establish a clear distinction between **SIPr**, **IPr**, **IiPrMe$_2$**, and **CAAC2**. However, this group of carbenes is clearly more electron donating than **diMe-IDM**, and less electron donating than **CAAC1** and especially **CAAC3**.

All of the ligands displayed in Chart 2 are collected again in Table 2 according to their calculated TEP. The first PA of each of them was computed as described by Frenking.[32] Although the great trends are respected, the correlation between the TEP and the PA, which does not take steric effects nor the backbonding into account, is not great (r^2 = 0.9283, plot not shown). For instance, ***i*Pr$_2$NH** is intrinsically a better σ-donor than **DMAP** according to PA. Yet, its larger steric demand make it a "weaker" ligand to $Ni(CO)_3$ compared to **DMAP**. The same conclusion can be reached when comparing ***t*BuPCl$_2$** with **THF**. In addition to a larger steric hindrance, ***t*BuPCl$_2$** is a strong π-acceptor which limits the backbonding from Ni to CO compared to **THF**.

Table 2 also shows the experimental and calculated sum of the Cl−Ga−Cl angles. The calculated values are systematically larger than the experimental ones.[64] However, the difference proves relatively constant throughout the ligand series, which shows a reasonable linear correlation between the two data sets (Figure 7, r^2 = 0.9689 with **PPh_3-**, **Me_3PO-**, and **CAAC3-$GaCl_3$** excluded because of the quite large *R*-factor of the X-ray analyses).

Another way to confront the experimental sum of the Cl−Ga−Cl angles with a computed parameter is to use the antisymmetric stretching of the Ga−Cl bond. As mentioned

dx.doi.org/10.1021/ic401817g | *Inorg. Chem.* 2013, 52, 11493−11502

Table 2. $LNi(CO)_3$ Tolman Electronic Parameter (TEP), Proton Affinity of L (PA), Sum of Cl−Ga−Cl Angles in $L{\cdot}GaCl_3$, Average Antisymmetric Stretching of $GaCl_3$ in $L{\cdot}GaCl_3$, and Percent Buried Volume of L in $L{\cdot}GaCl_3$ ($\%V_{bur}$)

L	TEP (cm^{-1})[a] calcd, scaled	PA[b] calcd, unscaled	Σ_{ClGaCl} (deg)[c] exp.	Σ_{ClGaCl} (deg)[d] calcd	$\nu_{GaCl}(E)$ (cm^{-1})[e] calcd, unscaled	$\%V_{bur}$[f]
$tBuPCl_2$	2087.9	202.3	340.1(1)	349.54	418.6	34.4
THF	2081.2	195.8	340.8(1)	351.20	422.5	19.7
Me_3SiN_3	2079.0	192.6	340.1(3)	348.79	417.4	23.3
Me_3PO	2071.7	218.7	332.4(3)	344.11	406.0	17.2[g]
N_3P_2	2070.6	-[h]	337.4(2)	346.49	411.0	20.2
3,5-Me_2Py	2068.5	225.9	335.86(6)	346.60	408.6	20.9
Pip	2068.0	226.7	337.02(6)	348.04	411.1	21.6
PPh_3	2067.5	231.2	336.6(2)	342.90	399.6	36.2
DMAP	2065.8	236.9	334.9(1)	345.27	407.7	20.6
iPr_2NH	2066.0	230.0	331.5(2)	342.27	405.1	29.7
PEt_3	2062.7	232.0	330.91(6)	341.52	397.4	35.8
PPr_3	2061.6	234.7	328.82(6)	341.13	396.6	34.8
N_2B	2060.4	239.5	330.18(9)	338.00	400.0	-[i]
diMe-IDM	2054.1	260.6	325.33(6)	337.09	390.8	26.1
SIPr	2051.5	-[h]	323.93(6)	333.35	388.0	38.1
IPr	2050.5	-[h]	324.20(8)	333.39	387.2	37.2
CAAC1	2050.0	270.5	321.47(9)	333.79	384.4	41.0
IiPrMe$_2$	2049.6	271.5	322.6(2)	333.10	383.0	27.8
CAAC2	2049.0	272.4	324.09(3)	333.06	382.2	40.9
CAAC3	2046.3	272.5	318.9(2)	326.08	378.5	44.8
1	2039.0	282.1	319.74(1)	329.24	372.3	39.0
2	2034.9	284.5	315.97(3)	329.05	367.0	40.4
3	2032.0[j]	*h*	315.40(3)	326.82	364.5	41.3
4	2031.9[j]	281.7	312.64(3)	327.03	365.1	38.0
5	2026.7	281.0	310.85(8)	325.3	361.0	34.8

[a]Obtained from the optimized $LNi(CO)_3$ complexes at the mPW1PW91/6-311+G(2d) (Ni)/6-311+G(d,p) (other atoms) level of theory (TEP = $\nu_{CO}(A1)*0.9541$). [b]First PA in kcal/mol at the BP86-def2-SVP//MP2-def2-TZVPP level of theory. [c]Obtained from the X-ray structures of $L{\cdot}GaCl_3$ complexes, average value when two molecules are found existing in the unit cell. [d]Calculated at the BP86/def2-SVP level of theory. [e]Antisymmetric stretching obtained from the optimized $L{\cdot}GaCl_3$ complexes at the BP86-def2-SVP level of theory, average of two values for all compounds except **CAAC3-$GaCl_3$** which shows three antisymmetric stretching mode of the Ga−Cl bond (unscaled). [f]Calculated from the ligand coordinates derived from the X-ray analysis of the $L{\cdot}GaCl_3$ complex by placing the center of the sphere at 2.0 Å from the donor atom, H atoms omitted except for secondary amines, average value when two molecules are found existing in the unit cell. [g]The three carbon atoms were used for the axis definition. [h]Too large to allow MP2 calculation. [i]Cannot be calculated since the boron atom is not implemented in SambVca. [j]Obtained from the optimized $LNi(CO)_3$ complexes at the BP86-def2-SVP level of theory (TEP = $\nu_{CO}(A1)*1.0472-109.94$).

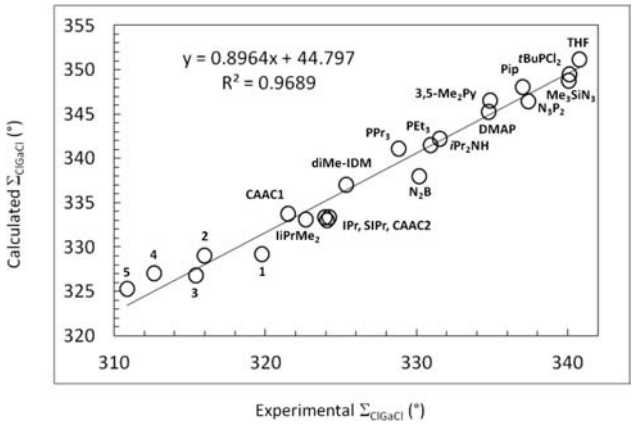

Figure 7. Plot of calculated vs experimental Σ_{ClGaCl} values.

above, it would be difficult to get a precise measurement by IR spectroscopy. Nevertheless, computed gas phase IR frequencies usually show a good linear correlation with experimental values. Thus, if the geometry of the gallium complex reflects the properties of the ligand, one expects a linear relationship with the calculated wavenumbers. The Ga−Cl bonds should become weaker as the donor strength of the ligand increases.[65] This trend is indeed nicely respected, as shown in Figure 8 (r^2 = 0.9788 with **PPh_3-**, **Me_3PO-**, and **CAAC3-$GaCl_3$** excluded).

Because nickel in the $Ni(CO)_3$ moiety is made electron-poor by the three carbonyl ligands, the Ni→L electron back-donation to ligands that are moderately π-basic is limited.[66] Besides, since the van der Waals volumes of $Ni(CO)_3$ and $GaCl_3$ are relatively similar,[67] and also because E−Ni and E−Ga bonds are in the same range (E = C, N, O, P; ∼ 2 Å), the two

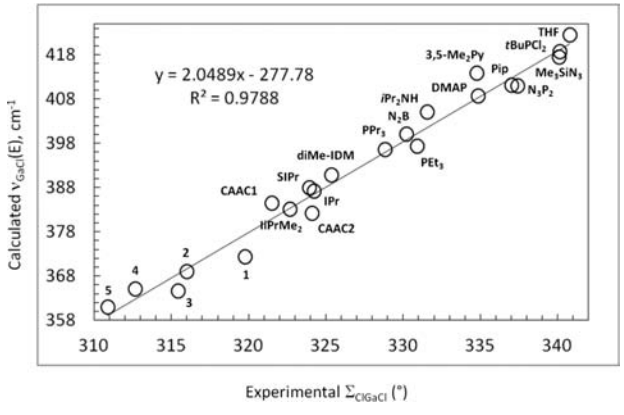

Figure 8. Plot of experimental Σ_{ClGaCl} values vs calculated $\nu_{GaCl}(E)$.

dx.doi.org/10.1021/ic401817g | Inorg. Chem. 2013, 52, 11493−11502

fragments should be similarly affected by the steric demand of the ligand. Therefore, a relatively good agreement between the $\nu_{CO}(A1)$ of the $LNi(CO)_3$ complexes and the sum of the Cl−Ga−Cl angles in the $L{\cdot}GaCl_3$ complexes can be expected. The plot of the calculated and scaled $\nu_{CO}(A1)$ vs the experimental Σ_{ClGaCl} shows indeed a good correlation between the two data sets (Figure 9, r^2 = 0.978 with **PPh_3-**, **Me_3PO-**, and **CAAC3-$GaCl_3$** excluded). ***t*BuPCl$_2$-GaCl$_3$** has also been excluded from the regression analysis. The latter is clearly a strong π-acceptor and should receive significant back-donation from nickel despite the three π-acidic carbonyls. Since back-bonding is not possible with gallium, a discrepancy is not surprising.

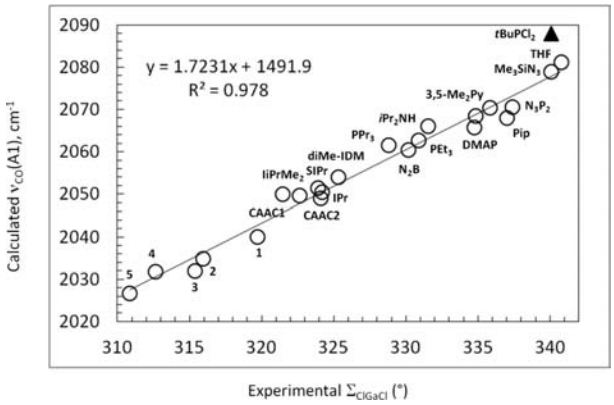

Figure 9. Plot of calculated TEP vs experimental Σ_{ClGaCl} values.

As expected, the nitrogen and the phosphorus donors give rise to a lower pyramidalization than NHC and CAAC ligands, and the *carbone* family promotes the larger one. In the phosphine series, the expected order is found: ***t*BuPCl$_2$** < **PPh_3** < **PEt_3** < **PPr_3**. The same is true for the oxygen donors: **THF** < **Me_3PO**. The classification of the amines according to the gallium scale is **Pip** < **3,5-Me_2Py** < **DMAP** < ***i*Pr$_2$NH**. This is not the same as that derived from the TEP, **3,5-Me_2Py** < **Pip** < **DMAP** < ***i*Pr$_2$NH**, nor that resulting from the PA, **3,5-Me_2Py** < **Pip** < ***i*Pr$_2$NH** < **DMAP**.[68] Although these three scales do not have to produce the same results, one can notice that ligands of the same class (i.e., secondary amines and pyridine derivatives) are found in the natural order: **Pip** < ***i*Pr$_2$NH**, and **3,5-Me_2Py** < **DMAP**. As mentioned above, the expected order of donation for the carbenes should be **diMe-IDM** < [**SIPr**, **IPr**, **IiPrMe$_2$**, **CAAC2**] < **CAAC1** < **CAAC3**, with some uncertainties regarding those in brackets. The gallium scale respects this trend, **diMe-IDM** < [**IPr** < **CAAC2** < **SIPr** < **IiPrMe$_2$**] < **CAAC1** < **CAAC3**, and also predicts the right donation order for the *carbones*: **1** < **2** < **3** < **4** < **5**.

In terms of electronic effect, the present gallium scale captures mostly the σ-donation property of the ligand. Thus, we checked the correlation between the Cl−Ga−Cl angles and the first PA. As for the response of the TEP vs PA (vide supra), the correlation coefficient is not great (r^2 = 0.9042 with **PPh_3-**, **Me_3PO-**, and **CAAC3-$GaCl_3$** excluded, plot not shown). We attribute this discrepancy to the fact that steric effects are mostly ignored by the PA. As stated by Clavier and Nolan,[35] electronic and steric effects are intimately related and difficult to separate. To quantify the steric hindrance brought about by the ligand to the $GaCl_3$ moiety, the percent buried volume was calculated from the coordinates of the solid state structures of the $L{\cdot}GaCl_3$ adducts.[35,69] Clearly there is no obvious relationship between the pyramidalization of the $GaCl_3$ moiety in the complexes and the steric demand of the ligands (r^2 = 0.5534, plot not shown). For instance, ligand **5** has a relatively modest $\%V_{bur}$ and yet the largest pyramidalization of the series was found for **5-$GaCl_3$**. Therefore, Σ_{ClGaCl} does not only reflect steric compression but mostly the σ-donation property of the ligand.

CONCLUSION

In this paper, we present the synthesis and structural characterization of rare molecular adducts of $GaCl_3$ with strong donor ligands of the *carbone* and CAAC families. In the solid state, the geometry of the $GaCl_3$ moiety obeys the electronic properties and the steric demand of the ligand. In agreement with Bent's rule, a stronger donor will concentrate the p character of the gallium orbitals toward the chlorine atoms, hence the compacting of the three Cl−Ga−Cl angles. While this rule has been sporadically used to compare related ligands together, no general scale has been based on geometrical features. However, we have shown that at least for a series of 26 $L{\cdot}GaCl_3$ complexes, and in spite of a narrow range of about 30° in the sum of the Cl−Ga−Cl angles, a good prediction of the electronic properties can be made. The use of this gallium scale in Ga(III) catalysis will be reported in due course.

ASSOCIATED CONTENT

Supporting Information

Crystallographic information files (CIFs). Coordinates and energies of the computed species. This material is available free of charge via the Internet at http://pubs.acs.org.

AUTHOR INFORMATION

Corresponding Author

*E-mail: vincent.gandon@u-psud.fr. Phone: +33 169 153 931. Fax: +33 169 154 747.

Notes

The authors declare no competing financial interest.

ACKNOWLEDGMENTS

We thank UPS (chaire d'excellence) and CNRS for financial support. V.G. is a member of the Institut Universitaire de France (IUF). We used the computing facility of the CRIHAN (project 2006-013).

REFERENCES

(1) (a) Dagorne, S.; Atwood, D. A. *Chem. Rev.* **2008**, *108*, 4037. (b) *The Group 13 Metals Aluminum, Gallium, Indium and Thallium: Chemical Patterns and Peculiarities*; Aldridge, S., Downs, A. J., Eds; John Wiley & Sons: Chichester, U.K., 2011.

(2) (a) Power, P. P. *Nature* **2010**, *463*, 171. (b) Summerscales, O. T.; Fettinger, J. C.; Power, P. P. *J. Am. Chem. Soc.* **2011**, *133*, 11960. (c) Power, P. P. *Acc. Chem. Res.* **2011**, *44*, 627.

(3) (a) Bonyhady, S. J.; Collis, D.; Frenking, G.; Holzmann, N.; Jones, C.; Stasch, A. *Nat. Chem.* **2010**, *2*, 865. (b) Holzmann, N.; Stasch, A.; Jones, C.; Frenking, G. *Chem.—Eur. J.* **2011**, *17*, 13517.

(4) (a) Ueng, S.-H.; Makhlouf Brahmi, M.; Derat, E.; Fensterbank, L.; Lacôte, E.; Malacria, M.; Curran, D. P. *J. Am. Chem. Soc.* **2008**, *130*, 10082. (b) Curran, D. P.; Solovyev, A.; Makhlouf Brahmi, M.; Fensterbank, L.; Malacria, M.; Lacôte, E. *Angew. Chem., Int. Ed.* **2011**, *50*, 10294. (c) Tehfe, M.-A.; Monot, J.; Malacria, M.; Fensterbank, L.; Fouassier, J.-P.; Curran, D. P.; Lacôte, E.; Lalevée, J. *ACS Macro Lett.* **2012**, *1*, 92.

(5) See inter alia: (a) Zhou, H.; Campbell, J. E.; Nguyen, S. T. *Org. Lett.* **2001**, *3*, 2229. (b) Buffet, J.-C.; Okuda, J.; Arnold, P. L. *Inorg.*

Chem. **2010**, *49*, 419. (c) Suzuki, T.; Atsumi, J.-i.; Sengoku, T.; Takahashi, M.; Yoda, H. *J. Organomet. Chem.* **2010**, *695*, 128. (d) Li, Z.; Plancq, B.; Ollevier, T. *Chem.—Eur. J.* **2012**, *18*, 3144. (e) Qiu, R.; Yin, S.; Song, X.; Meng, Z.; Qiu, Y.; Tan, N.; Xu, X.; Luo, S.; Dai, F.-R.; Au, C.-T.; Wong, W.-Y. *Dalton Trans.* **2011**, *40*, 9482. (f) Lamberti, M.; D'Auria, I.; Mazzeo, M.; Milione, S.; Bertolasi, V.; Pappalardo, D. *Organometallics* **2012**, *31*, 5551. (g) Bakewell, C.; Platel, R. H.; Cary, S. K.; Hubbard, S. M.; Roaf, J. M.; Levine, A. C.; White, A. J. P.; Long, N. J.; Haaf, M.; Williams, C. K. *Organometallics* **2012**, *31*, 4729. (h) Tian, D.; Liu, B.; Zhang, L.; Wang, X.; Zhang, W.; Han, L.; Park, D.-W. *J. Ind. Eng. Chem.* **2012**, *18*, 1332. (i) Jiang, W.; Gorden, J. D.; Goldsmith, C. R. *Inorg. Chem.* **2013**, *52*, 5814.

(6) For a discussion, see: Fey, N.; Haddow, M. F.; Harvey, J. N.; McMullin, C. L.; Orpen, A. G. *Dalton Trans.* **2009**, 8183.

(7) On the other hand, the contribution of π-donation is important for instance in LMX_2^+ complexes where M is a Group 13 element with one vacant orbital, or in neutral $LBeCl_2$ complexes since beryllium has two formally vacant valence orbitals, see respectively: (a) Inés, B.; Patil, M.; Carreras, J.; Goddard, R.; Thiel, W.; Alcarazo, M. *Angew. Chem., Int. Ed.* **2011**, *50*, 8400. (b) Petz, W.; Dehnicke, K.; Holzmann, N.; Frenking, G.; Neumüller, B. *Z. Anorg. Allg. Chem.* **2011**, *637*, 1702.

(8) The first PA is defined as the enthalpy difference between a neutral compound and the corresponding protonated species at 298 K. The second PA corresponds to the addition of a second proton to the monoprotonated species.

(9) (a) Li, H.-J.; Guillot, R.; Gandon, V. *J. Org. Chem.* **2010**, *75*, 8435. (b) Tang, S.; Monot, J.; El-Hellani, A.; Michelet, B.; Guillot, R.; Bour, C.; Gandon, V. *Chem.—Eur. J.* **2012**, *18*, 10239.

(10) For (NHC)·$GaCl_3$ complexes, see ref 9b and (a) Stasch, A.; Singh, S.; Roesky, H. W.; Noltemeyer, M.; Schmidt, H.-G. *Eur. J. Inorg. Chem.* **2004**, 4052. (b) Marion, N.; Escudo-Adán, E. C.; Benet-Buchholz, J.; Stevens, E. D.; Fensterbank, L.; Malacria, M.; Nolan, S. P. *Organometallics* **2007**, *26*, 3256. (c) El-Hellani, A.; Monot, J.; Guillot, R.; Bour, C.; Gandon, V. *Inorg. Chem.* **2013**, *52*, 506.

(11) (a) Kaufhold, O.; Hahn, F. E. *Angew. Chem., Int. Ed.* **2008**, *47*, 4057. (b) Petz, W.; Frenking, G. *Top. Organomet. Chem.* **2010**, *30*, 49. (c) Melaimi, M.; Soleihavoup, M.; Bertrand, G. *Angew. Chem., Int. Ed.* **2010**, *49*, 8810. (d) Martin, D.; Melaimi, M.; Soleihavoup, M.; Bertrand, G. *Organometallics* **2011**, *30*, 5304. (e) Alcarazo, M. *Dalton Trans.* **2011**, 1839.

(12) El-Hellani, A.; Bour, C.; Gandon, V. *Adv. Synth. Catal.* **2011**, *353*, 1865.

(13) Zeng, X.; Kinjo, R.; Donnadieu, B.; Bertrand, G. *Angew. Chem., Int. Ed.* **2010**, *49*, 942.

(14) (a) Kaska, W. C.; Mitchell, D. K.; Reichelderfer, R. F. *J. Organomet. Chem.* **1973**, *47*, 391. (b) Tonner, R.; Öxler, F.; Neumüller, B.; Petz, W.; Frenking, G. *Angew. Chem., Int. Ed.* **2006**, *45*, 8038. (c) Tonner, R.; Frenking, G. *Angew. Chem., Int. Ed.* **2007**, *46*, 8695. (d) Dyker, C. A.; Lavallo, V.; Donnadieu, B.; Bertrand, G. *Angew. Chem., Int. Ed.* **2008**, *47*, 3206. (e) Schmidbaur, H.; Schier, A. *Angew. Chem., Int. Ed.* **2013**, *52*, 176.

(15) (a) Schmidbaur, H.; Zybill, C. E.; Müller, G.; Krüger, C. *Angew. Chem., Int. Ed. Engl.* **1983**, *22*, 729. (b) Vicente, J.; Singhal, A. R.; Jones, P. G. *Organometallics* **2002**, *21*, 5887.

(16) Alcarazo, M.; Lehmann, C. W.; Anoop, A.; Thiel, W.; Fürstner, A. *Nat. Chem.* **2009**, *1*, 295.

(17) (a) Ramirez, F.; Desai, N. B.; Hansen, B.; McKelvie, N. *J. Am. Chem. Soc.* **1961**, *83*, 3539. (b) Appel, R.; Knoll, F.; Schöler, H.; Wihler, H.-D. *Angew. Chem., Int. Ed. Engl.* **1976**, *15*, 702.

(18) (a) Schmidbaur, H.; Costa, T.; Milewski-Mahrla, B.; Schubert, U. *Angew. Chem., Int. Ed. Engl.* **1980**, *19*, 555. (b) Schmidbaur, H.; Costa, T. *Chem. Ber.* **1981**, *114*, 3063. (c) Schubert, U.; Kappenstein, C.; Milewski-Mahrla, B.; Schmidbaur, H. *Chem. Ber.* **1981**, *114*, 3070.

(19) Fürstner, A.; Alcarazo, M.; Krause, H.; Wipf, P.; Deutsch, C. *Org. Synth.* **2009**, *86*, 298.

(20) (a) Esterhuysen, C.; Frenking, G. *Chem.—Eur. J.* **2011**, *17*, 9944. (b) Tonner, R.; Frenking, G. *Chem.—Eur. J.* **2008**, *14*, 3260. (c) Tonner, R.; Frenking, G. *Chem.—Eur. J.* **2008**, *14*, 3273. (d) Fürstner, A.; Alcarazo, M.; Goddard, R.; Lehmann, C. W. *Angew. Chem., Int. Ed.* **2008**, *47*, 3210.

(21) Petz, W.; Kutschera, C.; Tsan, S.; Weller, F.; Neumueller, B. *Z. Anorg. Allg. Chem.* **2003**, *629*, 1235.

(22) (a) Monot, J.; Fensterbank, L.; Malacria, M.; Lacôte, E.; Geib, S. J.; Curran, D. P. *Beilstein J. Org. Chem.* **2010**, *6*, 709. (b) Frey, G. D.; Masuda, J. D.; Donnadieu, B.; Bertrand, G. *Angew. Chem., Int. Ed.* **2010**, *49*, 9444. (c) Braunschweig, H.; Chiu, C.-W.; Damme, A.; Ferkinghoff, K.; Kraft, K.; Radacki, K.; Wahler, J. *Organometallics* **2011**, *30*, 3210.

(23) Lavallo, V.; Canac, Y.; Präsang, C.; Donnadieu, B.; Bertrand, G. *Angew. Chem., Int. Ed.* **2005**, *44*, 5705.

(24) Sheldrick, G. M. *SHELXS-97, Program for Crystal Structure Solution*; University of Göttingen: Göttingen, Germany, 1997.

(25) Sheldrick, G. M. *SHELXL-97, Program for the refinement of crystal structures from diffraction data*; University of Göttingen: Göttingen, Germany, 1997.

(26) Farrugia, L. J. *J. Appl. Crystallogr.* **1999**, *32*, 837.

(27) Flack, H. D. *Acta Crystallogr.* **1983**, *A39*, 876.

(28) Frisch, M. J. et al.; *Gaussian 03*, Revision C.02; Gaussian, Inc.: Wallingford, CT, 2004.

(29) (a) Møller, Chr.; Plesset, M. S. *Phys. Rev.* **1934**, *46*, 618. (b) Binkley, J. S.; Pople, J. A. *Intern. J. Quantum Chem.* **1975**, *9*, 229.

(30) (a) Becke, A. D. *Phys. Rev. A* **1988**, *38*, 3098. (b) Perdew, J. P. *Phys. Rev. B* **1986**, *33*, 8822.

(31) Weigend, F.; Ahlrichs, R. *Phys. Chem. Chem. Phys.* **2005**, *7*, 3297.

(32) Tonner, R.; Heydenrych, G.; Frenking, G. *ChemPhysChem* **2008**, *9*, 1474. The resolution-of-identity method has not been applied in our case, hence some slight differences between our values and the reported ones for **diMe-IDM**, **3**, and **4**.

(33) Gusev, D. G. *Organometallics* **2009**, *28*, 6458.

(34) Tonner, R.; Frenking, G. *Organometallics* **2009**, *28*, 3901.

(35) Clavier, H.; Nolan, S. P. *Chem. Commun.* **2010**, 841.

(36) (a) Gandon, V.; Lemière, G.; Hours, A.; Fensterbank, L.; Malacria, M. *Angew. Chem., Int. Ed.* **2008**, *47*, 7534. (b) Fensterbank, L.; Malacria, M.; Gandon, V. In *Topics in Current Chemistry*; Soriano, E., Marco-Contelles, J., Eds.; Springer-Verlag: Berlin, Germany, 2011; Vol. *302*, p 157.

(37) See inter alia: (a) Tolman, C. A. *Chem. Rev.* **1977**, *77*, 313. (b) Perrin, L.; Clot, E.; Eisenstein, O.; Loch, J.; Crabtree, R. H. *Inorg. Chem.* **2001**, *40*, 5806. (c) Chianese, A. R.; Li, X.; Janzen, M. C.; Faller, J. W.; Crabtree, R. H. *Organometallics* **2003**, *22*, 1663. (d) Kühl, O. *Coord. Chem. Rev.* **2005**, *249*, 693. (e) Crabtree, R. H. *J. Organomet. Chem.* **2005**, *690*, 5451. (f) Herrmann, W. A.; Schütz, J.; Frey, G. D.; Herdtweck, E. *Organometallics* **2006**, *25*, 2437. (g) Fey, N.; Tsipis, A. C.; Harris, S. E.; Harvey, J. N.; Orpen, A. G.; Mansson, R. A. *Chem.—Eur. J.* **2006**, *12*, 291. (h) Díez-González, S.; Nolan, S. P. *Coord. Chem. Rev.* **2007**, *251*, 874. (i) Fürstner, A.; Alcarazo, M.; Krause, H.; Lehmann, C. W. *J. Am. Chem. Soc.* **2007**, *129*, 12676. (j) Pombeiro, A. J. L. *Eur. J. Inorg. Chem.* **2007**, 1473. (k) Kelly, R. A., III; Clavier, H.; Guidice, S.; Scott, N. M.; Stevens, E. D.; Bordner, J.; Samardjiev, I.; Hoff, C. D.; Cavallo, L.; Nolan, S. P. *Organometallics* **2008**, *27*, 202. (l) Gusev, D. G. *Organometallics* **2009**, *28*, 763. (m) Huynh, H. V.; Han, Y.; Jothibasu, R.; Yang, J. A. *Organometallics* **2009**, *28*, 5395. (n) Dröge, T.; Glorius, F. *Angew. Chem., Int. Ed.* **2010**, *49*, 6940.

(38) For information about gallium NMR, see: Cheng, F.; Hector, A. L.; Levason, W.; Reid, G.; Webster, M.; Zhang, W. *Inorg. Chem.* **2007**, *46*, 7215.

(39) Greenwood, N. N.; Srivastava, T. S.; Straughan, B. P. *J. Chem. Soc. (A), Inorg. Phys. Theor.* **1966**, 699.

(40) Dauber, P.; Hagler, A. T. *Acc. Chem. Res.* **1980**, *13*, 105.

(41) Timoshkin, A. Y.; Bodensteiner, M.; Sevastianova, T. N.; Lisovenko, A. S.; Davydova, E. I.; Scheer, M.; Graßl, C.; Butlak, A. V. *Inorg. Chem.* **2012**, *51*, 11602.

(42) (a) Bent, H. A. *J. Chem. Educ.* **1960**, *37*, 616. (b) Bent, H. A. *Chem. Rev.* **1961**, *61*, 275. (c) Huheey, J. E. *Inorg. Chem.* **1981**, *20*, 4033. (d) Jonas, V.; Boehme, C.; Frenking, G. *Inorg. Chem.* **1996**, *35*, 2097.

(43) For a discussion on the influence of the donor strength of ligands on the bond angles and the pyramidalization of halides of type $[MX_2L]_2$ where M is Al or Ga, and the different contribution of s- and p-orbitals, see: (a) Schnepf, A.; Doriat, C.; Möllhausen, E.; Schnöckel, H. *Chem. Commun.* **1997**, 2111. (b) Ecker, A.; Friesen, M. A.; Junker, M. A.; Üffing, C.; Köppe, R.; Schnöckel, H. *Z. Anorg. Allg. Chem.* **1998**, *624*, 513.
(44) Holthausen, M. H.; Feldmann, K.-O.; Schulz, S.; Hepp, A.; Weigand, J. J. *Inorg. Chem.* **2012**, *51*, 3374.
(45) Scholz, S.; Lerner, H.-W.; Bolte, M. *Acta Crystallogr., Sect. E: Struct. Rep. Online* **2002**, *58*, m586.
(46) Kouvetakis, J.; McMurran, J.; Matsunaga, P.; O'Keeffe, M.; Hubbard, J. L. *Inorg. Chem.* **1997**, *36*, 1792.
(47) Herler, S.; Mayer, P.; Schmedt auf der Günne, J.; Schulz, A.; Villinger, A.; Weigand, J. J. *Angew. Chem., Int. Ed.* **2005**, *44*, 7790.
(48) Nogai, S.; Schmidbaur, H. *Dalton. Trans.* **2003**, 3165.
(49) Schmidbaur, H.; Nogai, S. *Z. Anorg. Allg. Chem.* **2004**, *630*, 2218.
(50) Pauls, J.; Chitsaz, S.; Neumüller, B. *Z. Anorg. Allg. Chem.* **2001**, *627*, 1723.
(51) Nogai, S.; Schmidbaur, H. *Inorg. Chem.* **2002**, *41*, 4770.
(52) Cheng, F.; Hector, A. L.; Levason, W.; Webster, M. *Private Communication*, 2009 (COTBUJ).
(53) Böck, B.; Braun, U.; Habareder, T.; Mayer, P.; Nöth, H. *Z. Naturforsch.* **2004**, *59b*, 681.
(54) Cheng, F.; Codgbrook, H. L.; Hector, A. L.; Levason, W.; Reid, G.; Webster, M.; Zhang, W. *Polyhedron* **2007**, *26*, 4147.
(55) Tolman, C. A. *J. Am. Chem. Soc.* **1970**, *92*, 2953.
(56) Dorta, R.; Stevens, E. D.; Scott, N. M.; Costabile, C.; Cavallo, L.; Hoff, C. D.; Nolan, S. P. *J. Am. Chem. Soc.* **2005**, *127*, 2485.
(57) Petz, W.; Weller, F.; Uddin, J.; Frenking, G. *Organometallics* **1999**, *18*, 619.
(58) With phosphines, this method is not as accurate as that of Gusev.
(59) The experimental TEP is not available for this series.
(60) Khramov, D. M.; Lynch, V. M.; Bielawski, C. W. *Organometallics* **2007**, *26*, 6042.
(61) Sato, T.; Hirose, Y.; Yoshioka, D.; Oi, S. *Organometallics* **2012**, *31*, 6995.
(62) Neveling, A.; Julius, G. R.; Cronje, S.; Esterhuysen, C.; Raubenheimer, H. G. *Dalton Trans.* **2005**, 181.
(63) Lavallo, V.; Canac, Y.; DeHope, A.; Donnadieu, B.; Bertrand, G. *Angew. Chem., Int. Ed.* **2005**, *44*, 7236.
(64) We also used the MP2 technique, various DFT functional (B3LYP, B3P86, M06, PBE1PBE0, or mPW1PW91), and larger basis sets (SVPD, TZVPP, or 6-311+G(d,p)). However, the calculated values did not change significantly.
(65) (a) Gutmann, V. *Coord. Chem. Rev.* **1975**, *15*, 207. (b) Gutmann, V. *The Donor-Acceptor Approach to Molecular Interactions*; Plenum Press: New York, 1977. (c) Jensen, W. B. *The Lewis Acid-Base Concept, an Overview*; Wiley and Sons: New York, 1980. (d) Denmark, S. E.; Beutner, G. L. *Angew. Chem., Int. Ed.* **2008**, *47*, 1560.
(66) Comas-Vives, A.; Harvey, J. N. *Eur. J. Inorg. Chem.* **2011**, 5025.
(67) $Ni(CO)_3$ and $GaCl_3$ were optimized at the BP86/def2-SVP level and superimposed in the Chemcraft software with the van der Waals spheres highlighted (http://www.chemcraftprog.com/).
(68) The pK_a values are not known for all ammoniums and not always available in the same solvent.
(69) Poater, A.; Cosenza, B.; Correa, A.; Giudice, S.; Ragone, F.; Scarano, V.; Cavallo, L. *Eur. J. Inorg. Chem.* **2009**, 1759.